Retinal Vessel Classification Based on Maximization of Squared-Loss Mutual Information

D. Relan, L. Ballerini, E. Trucco and T. MacGillivray

Abstract The classification of retinal vessels into arterioles and venules is important for any automated system for the detection of vascular changes in the retina and for the discovery of biomarkers associated with systemic diseases such as diabetes, hypertension, and cardiovascular disease. We introduce Squared-loss Mutual Information clustering (SMIC) for classifying arterioles and venules in retinal images for the first time (to the best of our knowledge). We classified vessels from 70 fundus camera images using only 4 colour features in zone B (802 vessels) and in an extended zone (1,207 vessels). We achieved an accuracy of 90.67 and 87.66 % in zone B and the extended zone, respectively. We further validated our algorithm by classifying vessels in zone B from two publically available datasets—INSPIRE-AVR (483 vessels from 40 images) and DRIVE (171 vessels from 20 test images). The classification rates obtained on INSPIRE-AVR and DRIVE dataset were 87.6 and 86.2 %, respectively. We also present a technique to sort the unclassified vessels which remained unlabeled by the SMIC algorithm.

Keywords Retinal · Fundus · Vessels · Arterioles · Venules · Classification · Clustering

D. Relan (✉) · T. MacGillivray
Centre for Clinical Brain Sciences, Edinburgh, UK
e-mail: devanjali.relan@ed.ac.uk

L. Ballerini · E. Trucco
School of Computing, University of Dundee, Dundee, UK

T. MacGillivray
Clinical Research Imaging Centre, University of Edinburgh, Edinburgh, UK

T. MacGillivray
Clinical Research Facility, University of Edinburgh, Edinburgh, UK

R. Singh et al. (eds.), *Machine Intelligence and Signal Processing*,
Advances in Intelligent Systems and Computing 390,
DOI 10.1007/978-81-322-2625-3_7

1 Introduction

The retina is the only location in the human body where blood vessels can be directly visualized non-invasively in vivo. Many important eye diseases as well as systemic diseases such as diabetes and hypertension manifest themselves in the retina [1]. Quantitative structural analysis of the retinal vasculature helps in the diagnosis of retinopathies as well as providing candidate biomarkers of systemic diseases. The vascular changes during the onset of a systemic disease can affect very differently arteries and veins. For example, one of the early signs of retinopathy is generalized arteriolar narrowing [2], i.e. a decrease in the ratio between arteriolar and venular diameters (AVR). There is also mounting evidence that narrowed retinal arterioles are associated with long-term risk of hypertension, while AVR is a well-established predictor of stroke and other cardiovascular events [3, 4]. In order to realize an automatic tool such as VAMPIRE (Vasculature Assessment and Measurement Platform for Images of the REtina) [5] for vasculature characterization, it is highly desirable to automatically distinguish vessels as arterioles and venules.

Conventionally, AVR and other measurements of retinal vascular parameters are measured from zone B—an annulus 0.5 to 1 optic disc (OD) diameter from the OD boundary [2–4] and this region has been used for the investigation of retinal biomarkers in several studies [2, 4, 6]. However, measurements from outside this zone might also lead to candidate biomarkers of disease. For instance, Cheung et al. studied the association of blood pressure with retinal vascular caliber measured over the standard zone B and an extended zone of the fundus images [7]. They found that the reliability of retinal vascular caliber measurements was high for the extended zone.

We propose an automatic unsupervised retinal vessel clustering method based on Squared-loss Mutual Information (SMIC) [8] for the first time (to the best of our knowledge). We tested this on vessels in zone B and an extended zone using 4 fixed features frequently chosen or selected automatically as discriminative features for vessel classification [9].

Supervised vessel classification has previously been proposed in many studies [10–12], but this generally requires large volumes of clinical annotations on images. Therefore we attempt to classify vessels in unsupervised manner removing this burden. In our previous work [13], we proposed an unsupervised vessel classification method using a Gaussian Mixture Model with an Expectation-Maximization (GMM-EM) classifier. We demonstrated 92 % classification with 13.5 % unclassified vessels using a quadrant pair wise approach and 4 fixed features on 406 vessels from 35 images in zone B. We repeated the experiment on a further 35 images giving 70 images in total with 802 vessels and resulting in 90.45 % correct classification and with 13.8 % unclassified. The limitation of method was that it gave us a high percentage of unclassified vessels. In another study [14] we presented supervised a Least Square-Support Vector Machine (LS-SVM) classifier to label vessels automatically. The performance of our system was very promising and it only required a small

set of training images. But like other supervised method our LS-SVM classification framework needs new training data for every new image set.

In [15], vessel classification was performed on 58 images using K-Means clustering between two concentric circumferences around the OD. In their study quadrants were rotated in steps of 20° to include at least one artery and one vein in each quadrant. They reported 87 and 90.08 % correct classification before and after applying their proposed tracking method in [16]. In [17], quadrant-wise vessel classification was performed using fuzzy a C-Mean clustering method in a concentric zone around the OD on 443 vessels from 35 images. Their proposed method resulted in 87.6 % correct classification. In [18], fuzzy C-Mean clustering was applied on 15 images for vessel classification with 88.28 % classification accuracy.

In many of the previous studies the INSPIRE-AVR [10] and DRIVE [19] datasets were used to test supervised classifiers. The authors in [10] tested on the INSPIRE-AVR dataset to classify vessels in zone B with 27 features, and their proposed method gave the best result with Linear Discriminant Analysis (LDA) (area under ROC 0.84). Mirsharif et al. [11] evaluated the performance of their supervised classification method on two different datasets viz. DRIVE (40 retinal images) and their own dataset (13 retinal images) resulting in 90.2 and 88.2 % accuracy, respectively. Dashtbozorg et al. in [12] presented a combination of graph-based classification with feature selection using LDA to classify all vessel pixels in entire images. Their method resulted in accuracy values of 88.3, 87.4 and 89.8 % with INSPIRE-AVR (40 images), DRIVE (20 images) and VICAVR (58 images) dataset, respectively.

In order to validate the performance of our system we therefore selected to test our algorithm on the INSPIRE-AVR and DRIVE datasets.

2 Methodology

2.1 Material

70 colour fundus images were selected at random from a large database of non-mydriatic fundus images (Orkney Complex Disease Study—ORCADES). These images with resolution 2048 × 3072 pixels were captured with a Canon CR-DGi non- mydriatic retinal camera having 45º field of view. 802 vessels in zone B and 1,207 vessels in the extended zone were classified computationally. We also tested our algorithm on 171 vessels from 40 INSPIRE-AVR images and 483 vessels from 20 test DRIVE images.

Ground truth for the 70 ORCADES images was generated by two observers (authors DR and TM who were individually and independently trained by experienced clinicians in the identification of the retinal vessel type) by manual labelling vessels as arteriole or venule. Observer 1 (DR) is a doctoral student (less experienced, ~2.5 year); observer 2 (TM) is an imaging scientist and specialist of retinal image analysis (more experienced, >12 years).

2.2 Image Pre-processing

The hue channel was pre-processed to improve the contrast of vessels against background by mapping the original intensity values such that values between 0.01 and 0.8 map to values between 0 and 1. We then compensated for background illumination in red, green and re-mapped hue channels using Chrástek's method [20] as the presence of inter- and intra-image contrast, luminosity and colour variability affect classification performance.

2.3 Vessels and Features Extraction

Centerline pixels of vessels in zone B were extracted as previously reported [13], and vessels in the extended zone were extracted as reported in [14]. The image was divided into four quadrants by locating the OD and its diameter. Once the centerline pixels were found in each quadrant, four colour features—mean of red (MR), mean of green (MG), mean of hue (MH) and variance of red (VR)—were extracted from the illuminated corrected channels and from a circular neighborhood around each centerline pixel, with diameter 60 % of the mean vessel diameter.

After feature extraction, we have four sets of feature vectors $F_q, q = 1, \ldots, 4$, for each pair of quadrant—i.e. for pairs (I, II), (II, III), (III, IV) and (IV, I). Each set of colour features (F_q) of pixels were classified using the SMIC classifier. The classification was performed by working separately on two quadrants at a time in a clockwise direction, i.e. classification of vessels from quadrant combinations (I, II), (II, III), (III, IV) and (IV, I). The classifier labels each pixel as either arteriole or venule. Thereafter, labels were polled for all pixels in a vessel, and the winning vote used to assign the vessel status. If the vote was tied the vessel was marked unclassified. Vessels from ORCADES and DRIVE images were classified using four features (MR, MG, VR and MH) whereas INSPIRE-AVR images were classified using MR, MG and VR due to poor hue channel quality (see Fig. 1).

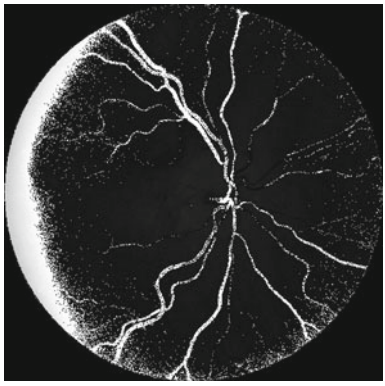

Fig. 1 Poor hue channel of image from INSPIRE-AVR dataset (image40.jpg)

2.4 Reducing Unclassified Vessels

In order to reduce the number of unclassified vessels the colour features of unclassified vessels were compared quadrant pair wise with that of classified arterioles and venules. Let each image have n vessels, i.e. $S = V_{1k}, V_{2k}, \ldots, V_{nk}$, where V_{ik} is ith vessel in kth quadrant. Each vessel is represented by a set of m centerline pixels: $V_{ik} = p_{1k}, p_{2k}, \ldots, p_{mk}$. On each centerline pixel of unclassified and classified vessels, MR and MG were extracted because MR and MG are dominating features to distinguish arterioles and venules [9]. The average of MR and MG from all centerline pixels of each of the vessel V_{ik} in all four quadrants ($k = 1, \ldots, 4$) were calculated separately for unclassified vessels (u), arteries (a) and veins (v). This gives [MGu MRu], [MGa MRa] and [MGv MRv]. Then, [MGu MRu] was compared with [MGa MRa] and [MGv MRv] quadrant pair wise in order to assign a label to the unlabeled vessel. For instance, first [MGu MRu] was compared with [MGa MRa] and [MGv MRv] in quadrant pair (I, II). If the absolute difference between [MGu, MRu] and [MGa, MRa], respectively is less than the absolute difference with [MGv, MRv], a soft label of *arteriole* was assigned. Alternatively if the absolute difference between [MGu, MRu] and [MGv, MRv] respectively is less than the absolute difference with [MGa, MRa], a soft label of *venule* was assigned. Likewise the color features of unclassified vessels were compared with that of classified arterioles and venules in remaining quadrant pairs (II, III), (III, IV) and (IV, I) assigning one more soft labels. Finally, each unclassified vessel was assigned a deciding label based on the polling of soft labels. If the vote was tied the vessel remained unclassified.

3 Results

Table 1 summarizes the results (where C is the percentage of correctly classified vessels and *Un* stands for the unclassified vessels, both w.r.t observer 1). The classification rates obtained with SMIC and GMM-EM were almost the same but the percentage of unclassified vessels with GMM-EM is higher compared to SMIC in zone B. Results were slightly higher as compared with observer 2. The classification rates obtained with SMIC in the extended zone were higher and unclassified vessels were lower as compared to GMM-EM.

Table 2 summarizes the classification results when we applied our algorithm to images from INSPIRE-AVR and DRIVE. SMIC outperforms GMM-EM in terms

Table 1 Classification rate on ORCADES dataset

Classifier	Zone B C/Un (%)	Extended zone C/Un (%)
SMIC [8]	90.67/6.48	87.66/5.89
GMM-EM [13]	90.45/13.8	84.74/13.44

Table 2 Classification rate on publically available dataset in Zone B

Classifier	INSPIRE-AVR C/Un (%)	DRIVE C/Un (%)
SMIC [8]	87.6/3.83	86.2/7
GMM-EM [13]	83.67/14	78.1/38.6

Table 3 Classification rate after applying method of reducing unclassified vessels

Classifier	Zone B C/Un (%)	Extended zone C/Un (%)
SMIC [8]	90.62/2.99	87.78/2.23
GMM-EM [13]	90.8/4.98	85.95/4.47

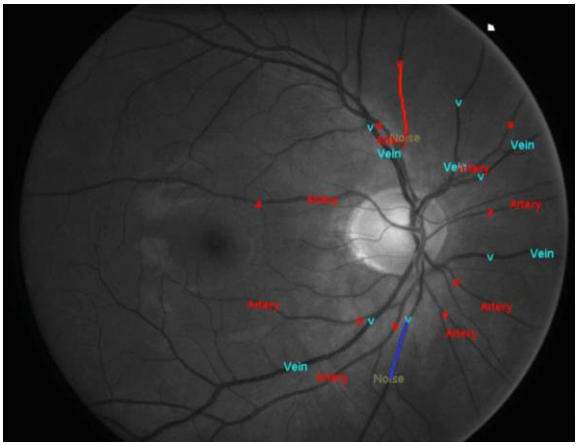

Fig. 2 Image showing vessel classification: 'v' and 'a' indicates ground truth of 'venule' and 'arterioles' respectively. Vessels marked with 'Vein' and 'Artery' is the classification outcome. 'Noise' are vessel that remain unlabeled. Vessels marked 'Noise' were assigned label 'arteriole' and 'venule' marked in *red* and *blue* respectively after applying our technique for classifying unlabeled vessels

of classification rate and percentage of unclassified vessels. Table 3 shows the result obtained after attempting to reduce the number of unclassified vessels. Figure 2 shows the classification result. There are two vessels which remain unlabeled by the SMIC algorithm and are marked 'Noise' in an image (see Fig. 2). Vessels marked in red and blue in Fig. 2 are 'arteriole' and 'venule' labels respectively assigned to unlabeled 'Noise' vessels after applying our technique for classifying unlabeled vessels.

4 Discussion and Conclusion

We have proposed a Squared-loss Mutual Information clustering (SMIC) method to cluster retinal vessels into arterioles and venules for the first time (to the best of our knowledge), using only four color features. The results were very promising in both zone B and in the extended zone. The performance of SMIC was better than that of the GMM-EM unsupervised classifier [13] both in terms of classification rate and

unclassified vessels for our dataset as well as publically available datasets. SMIC method clusters the data analytically via kernel eigenvalue decomposition and has advantage of finding the optimal solution. Unlike the previous information-maximization clustering methods, SMIC does not suffer from the problem of local optima. The classification percentage obtained by our system was higher than those reported in [15–18]. We analyzed 70 color fundus images compared to 58, 35 and 15 images analyzed in [16–18], respectively. The resolution of our images was 2048×3072 which is higher than 768×576, 1300×1000 and 800×1000 as used in [16–18], respectively. Therefore classification accuracy obtained by our system may differ with a different datasets. Moreover the classification rate is highly dependent on segmentation results (for extracting centerline pixels) and choice of retinal zone, classifier and framework. We validated the performance of our system on INSPIRE-AVR and DRIVE with classification rates of 87.6 and 86.2 %, respectively, which is higher than that obtained with GMM-EM. Our system resulted in a higher classification rate on INSPIRE-AVR when compared to [10] and close to that of [12]. On the DRIVE images the results obtained by our method was close to that of [12] and lower than that of [11]. However, it should be noted that the results in [10–12] are from supervised techniques and our method is unsupervised. Our method of reducing the unclassified vessels reduces the unlabeled vessels and increased the classification rate.

We conclude that our system performance is very promising. Further tests with much larger datasets are needed to declare suitability to support retinal vessel classification in biomarker research.

Acknowledgments This work is supported by Leverhulme Trust grant RPG-419 "Discovery of retinal biomarkers for genetics with large cross-linked datasets", and part of the VAMPIRE (Vasculature Assessment and Measurement Platform for Images of the REtina) project led by the University of Dundee and Edinburgh, UK [5]. We thank Dr. Jim Wilson, University of Edinburgh, for making the ORCADES images available.

References

1. Abràmoff, M.D., et al.: Retinal imaging and image analysis. IEEE Rev. Biomed. Eng. **3**, 169–208 (2010)
2. Wong, T.Y., et al.: Computer-assisted measurement of retinal vessel diameters in the Beaver Dam Eye Study: methodology, correlation between eyes, and effect of refractive errors. American academy of ophthalmology, pp. 90–1183 (2004)
3. Ikram, M.K., et al.: Retinal vessel diameters and risk of hypertension: the rotterdam study, hypertension. J. Am. Hear. Assoc. **47**(2), 94–189 (2006)
4. Leung, H., et al.: Relationships between age, blood pressure, and retinal vessel diameters in an older population. Investig. Ophthalmol Vis. Sci. **44**(7), 2900–2904 (2003)
5. Perez-Rovira, A., et al.: Vampire: vessel assessment and measurement platform for images of the retina. In: Proceedings of the IEEE Engineering in Medicine and Biology Society, pp. 3391–3394 (2011)
6. Li, H., Hsu, W., Lee, M., Wong, T.Y.: Automatic grading of retinal vessel calibre. IEEE Trans. Bio-med. Eng. **52**(7), 5–1352 (2005)

7. Cheung, C.Y.-L., Hsu, W., et al.: A new method to measure peripheral retinal vascular calibre over an extended area. Microcirculation **17**(7), 495–503 (2010)
8. Sugiyama, M., et al.: Information-Maximization Clustering based on Squared-Loss Mutual Information, pp. 40–20111
9. Jelinek, H.F., et al.: Towards vessel characterization in the vicinity of the optic disc in digital retinal images. In: Proceedings of the Image and vision computing (2005)
10. Niemeijer, M., Xu, X.: Automated measurement of the arteriolar-to-venular width ratio in digital color fundus photographs. IEEE Trans. Med. Imaging **30**(11), 50–1941 (2011)
11. Mirsharif, Q.: Automated characterization of blood vessels as arteries and veins in retinal images. Comput. Med. Imaging Graph. **37**(7–8), 17–607 (2013)
12. Dashtbozorg, B., et al.: An automatic graph-based approach for artery/vein classification in retinal images. IEEE Trans. Image Process. **23**(3), 1073–1083 (2014)
13. Relan, D., et al.: Retinal vessel classification: sorting arteries and veins. In: Conference Proceedings: Annual International Conference of the IEEE Engineering in Medicine and Biology Society, pp. 7396–7399 (2013)
14. Relan, D., et al.: Automatic retinal vessel classification using a least square-support vector machine in VAMPIRE'. In: 35th Annual International Conference of the IEEE EMBS Engineering in Medicine and Biology Society (EMBC), pp. 142–145. Chicago, USA (2014)
15. Saez, M., et al.: Development of an automated system to classify retinal vessels into arteries and veins. Comput. Methods programs Biomed. 1–10 (2012)
16. Vazquez, S.G., et al.: On the automatic computation of the Arterio-Venous Ratio in retinal images: using minimal paths for the Artery/Vein classification. In: International Conference on Digital Image Computing: Techniques and Applications, pp. 599–604 (2010)
17. Grisan, E., Ruggeri., A.: A divide et impera strategy for automatic classification of retinal vessels into arteries and veins, In: Proceedings of the 25th Annual International Conference of the IEEE Engineering in Medicine and Biology Society, pp. 890–893 (2003)
18. Joshi, V.S., et al.: Automated artery-venous classification of retinal blood vessels based on structural mapping method. In: Proceedings of the SPIE, vol. 8315 (2012)
19. Staal, J.J., Abramoff, M.D.: Ridge based vessel segmentation in color images of the retina. IEEE Trans. Med. Imaging **23**, 501–509 (2004)
20. Chrástek, R., et al.: Automated segmentation of the optic nerve head for diagnosis of glaucoma. Med. Image Anal. **9**(4), 297–314 (2005)